Volume 5, Issue 2, 2015, 932-936 **ISSN 2069-5837**

Biointerface Research in Applied Chemistry

www.BiointerfaceResearch.com

Review Article **Open Access Journal**

Received: 20.02.2015 / Revised: 15.03.2015 / Accepted: 25.03.2015 / Published on-line: 15.04.2015

Porous silicon nanowires: synthesis and applications

Mustapha Jouiad[1], Adel Najar[2*]

[1]Mechanical and Material Engineering Department, Masdar Institute of Science and Technology Abu Dhabi 54224, UAE

[2]NTT Basic Research Laboratories, NTT Corporation, 3-1, Morinosato-Wakamiya, Atsugi, Kanagawa 243-0198, Japan

*corresponding author e-mail address:*Adel.Najar@ntt.brl.co.jp*

ABSTRACT

High density vertically aligned Porous Silicon NanoWires (PSiNWs) were fabricated on silicon substrate using metal assisted chemical etching process. A linear dependency of nanowire length to the etching time was obtained and the change in the growth rate of PSiNWs by increasing etching durations was shown. A typical 3D TEM image for volume reconstruction of the sample shows the pores size varying from 10 to 50 nm.In this review, we present twoapplications of PSiNWs for gas detection and using surface-enhanced Raman spectroscopy (SERS) effect for organic molecules detection.

Keywords: *Porous Silicon NanoWires, gas detection, SERS, TEM, Electron tomography, 3D imaging.*

1. INTRODUCTION

Nanoscale silicon has been intensively investigated and explored for its applications in microelectronics, photonics, and biomedical sensors [1–3]. Specific efforts have been concentrated in the development of new silicon nanostructures, including quantum dots, nanowires, or porous silicon (PS). Porous silicon has attracted much attention, especially in enhancing photo-emission. Greatresearch efforts have been performed to realize an optical device with porous silicon [4–9], but the inefficiency [10] and instability [11] of optical characteristic in PS still remain. In addition, silicon nanowires (SiNWs) are also ideal candidate for the study of physics of low dimensional systems. It has potential impact in realizing nanoscale interconnects and functional device elements in future nanoscale electronic and optoelectronic devices [12, 13]. The field of SiNWs synthesis represents an exciting and rapidly expanding research area. Considerable efforts have been devoted to the development of versatile and controllable methods for the synthesis of SiNW. These methods can be broadly classified as: (i) bottom-up, and (ii) top-down approaches. The bottom-up approach involves the construction of desirable nanostructures from the basic components, i.e., from the atomic level to the nano- or micro-scale wires.

This method is useful for the fabrication of low-dimensional heterostructure based devices in large quantities [14-18]. Using bottom-up, SiNWs were first obtained by vapor–liquid–solid (VLS) method [19], followed by an etching step to create nanowires. The VLS method has been implemented in a variety of techniques, such as pulsed laser deposition (PLD) [20, 21], gas- phase molecular beam epitaxy (GS-MBE) [22], chemical vapor deposition (CVD) [23, 24], laser ablation [25, 26], and oxide assisted growth techniques [27]. Top-down approach seeks to fabricate SiNWs from high quality single crystal silicon wafer or thin film. Silicon nanowires have also been realized using lithographically defined patterns, or spin-coating of nanospheres as etched mask [28] followed by etching of the nanowires using plasma processing technique. MacEtch is a simple, cost-effective, and powerful semiconductor etching technique that is capable of producing high aspect ratio semiconductor nanostructures. By combining with metal patterning lithography or non-lithographic patterning methods, accurate control of the nanowire orientation (vertical vs slanted), size (nano vs microscale), shape, architecture, density, length, doping characteristics can be achieved readily at wafer scale.

The fabrication of silicon nanowires using the metal-assisted electroless etching method has also been adopted [29-33]. The silver (Ag) ions in an ionic solution of hydrofluoric acid (HF) and hydrogen peroxide (H_2O_2) have been used to prepare the arrays of SiNWs from single crystal wafers [34, 35]. The effects of various process parameters such as the etchant concentration of H_2O_2, etching time and post-etch treatment on the morphology and optical properties of the SiNWs have also been investigated [36]. The fabrication of nanowires using this method does not require complex sample preparation steps. Furthermore, this technique is effective, having high throughput and low cost.

In this review, we will present the synthesis process of PSiNWs and the structure properties. In the second time, we present two applications for these nanostructures as gas detector and SERS substrate for organic molecules detection.

2. EXPERIMENTAL SECTION

PSiNWs were fabricated by Ag assisted electroless etching method from n-type Si wafer (100) with a resistivity of 0.01–0.02 ohm cm. The Si wafers were cleaned using acetone followed by ethanol for 5min in an ultrasonic bath. Next, the wafers were immersed in a piranha solution H_2SO_4/ H_2O_2(3:1) for 20 min to remove the organic deposits from the surface. The cleaned wafers were transferred into HF/ $AgNO_3$ solution with a concentration of 4.8 M/0.005M for Ag-deposition, followed by rinsing with de-

ionized water. Then, the treated Si samples were etched in the HF/H_2O_2 solution for 45 min. Finally, samples were rinsed again for 10 min with HNO_3 solution to dissolve the excessive Ag nanoparticles (Ag NPs), leaving behind traces of Ag for catalyzing the etching reaction. Four samples were etched using HF concentration of 1.8, 2.8, 4.8, and 5.8 M, respectively, with a fixed H_2O_2concentration of 0.5 M.

3. RESULTS AND DISCUSSION SECTION

Figure 1(a) shows the scanning electron microcopy image of the vertically oriented PSiNWs having an average length of 13 μm after 75 min wet etching. The nanowires distribute uniformly on the sample. Figure 1(b) shows the top view with tips of NWs congregates together and the diameter of the congregated bundles is several micrometers. These congregated bundles are uniformly distributed on the entire samples and confirmed from the cross-section images. The transmission electron microscopy (TEM) image of an individual nanowire is shown Fig. 1(c), which shows that the nanowire has a diameter of ~150 nm.

A typical 3D-tomography observation was conducted using a TEM and 3D reconstructions were achieved using a simultaneous iterative reconstruction algorithm of consecutive 2D slices in Fig. 2(a). The pore sizes present a distribution from 10 to 50 nm, with an estimated measurement error of 10%, and these pores go inside the nanowire showing similar structure to porous silicon. An average distance between two neighboring pores of lower than 5 nm has been observed. These mesoporous structures are expected to show strong quantum confinement effects.

In the two-step chemical etching for highly doped Si wafers (n-type),[36-38] the silver nanoparticle catalysts are predeposited on the clean silicon surface. Since H_2O_2 itself cannot etch the silicon, the formation of porous structures needs to be facilitated by the metal nanoparticles. Previous studies suggested that the silver nanoparticles could be oxidized into Ag+ ion [34] during the etching process as follows:

$$2Ag + H_2O_2 + 2H^+ \rightarrow 2Ag^+ + 2H_2O$$

In a typical etch process, the silver particles are partially oxidized by H_2O_2 to create a localized Ag^+ cloud in the close proximity of the silver particles. Silver ions can quickly react with silicon and take electrons from silicon near the Ag/Si interface and be recovered into original silver particles again. In this way, the etching is localized around the silver nanoparticles and the silver nanoparticles are trapped in the nanopits created by themselves, leading to continued etching in the vertical direction and the formation ofvertical silicon nanowire array. However, as the H_2O_2 concentration increases, the concentration of Ag^+ ion increases. In this case, the Ag^+ ions may not be 100% recovered into the original silver nanoparticles and some of them may diffuse out.

When the amount of the out-diffused Ag^+ ions reach a certain threshold, they may nucleate on the side wall near defective sites (e.g., around the dopants) by extracting electrons from the silicon nanowires and forming new silver nanoparticles as a new etching pathway along the lateral direction of the nanowires.

In this way, the higher H_2O_2 concentration increases the amount of out-diffused Ag^+, and the increase of doping concentration increases the amount of weak defective points in the silicon lattice; both are important factors for the initiation of additional etching pathways in addition to the vertical etch, which explains the observation of the increased porositywith increasing H_2O_2 concentration during the etching of highly doped n-Si wafers.Figure 2(b) shows the length of the NWs versus the etching time. The length of PSiNWs is linear as a function of the etching time up to 190 min with an etching rate of 0.12 $\mu m.min^{-1}$. This clearly indicates the rapidity of the electroless etching process. On the other hand, beyond 190 min, we see a linear relationship, with a change in the etching rate of the nanowires lower than the expected for 460 min etching time. The etching rate of the nanowires between 190 and 460 was 0.01 $\mu m.min^{-1}$. This clearly indicates that the reaction slows down due to the decrease in the reaction kinetics. We attribute this to the inhibition of the sinking mechanism of Ag^+ ions to the bottom of the nanowire arrays, leading to a decrease in Ag^+ concentration. The drop in Ag concentration results in the deceleration of etching rate.

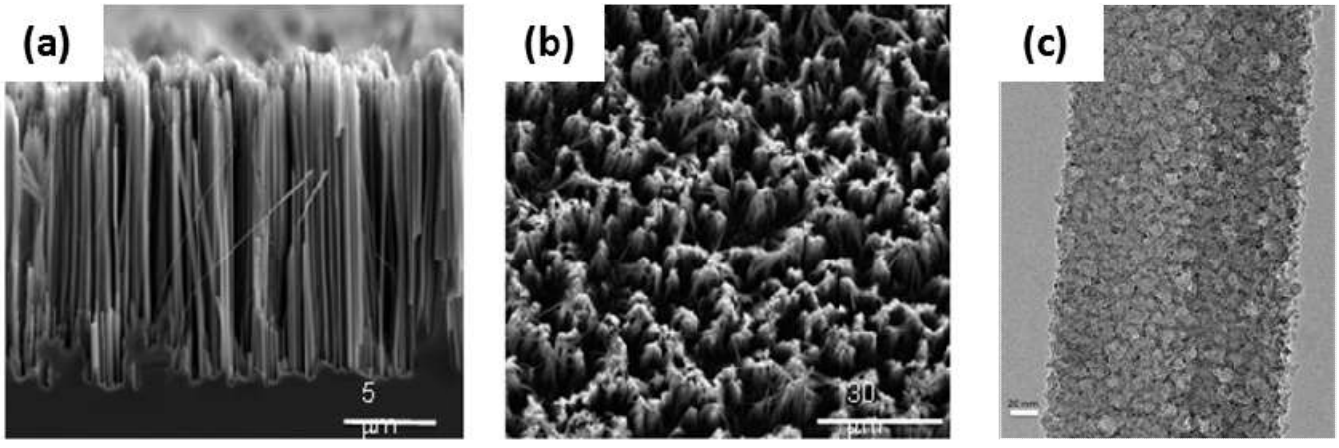

Figure 1. (a) Cross-section SEM micrograph of PSiNWs etched for 75 min, **(b)** top view micrograph of PSiNWs, **(c)** TEM image of individual nanowire and inset the FFT image. Reprinted with permission from [33]. Copyright (Journal of Applied Physics, 2012) AIP Publishing LLC.

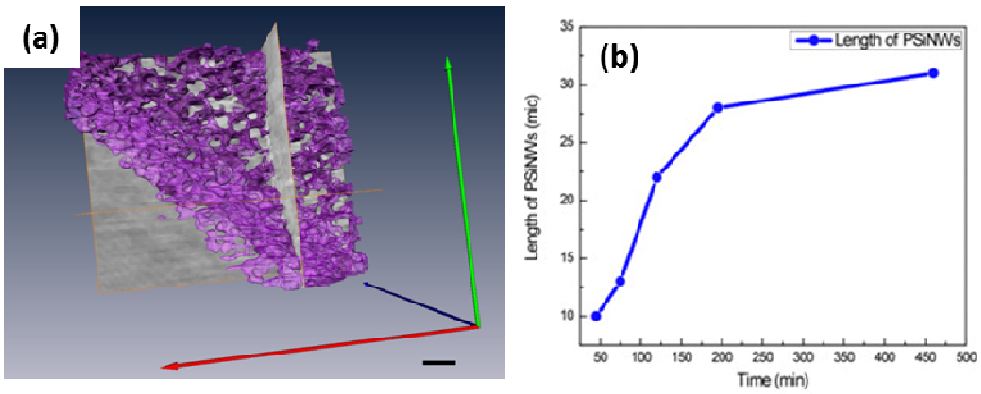

Figure 2. (a) 3D tomography TEM image of nanowires. **(b)**Variation of the nanowires length as a function of etching time 45 min, 75 min, 120 min, 195 min and 460 min.Reprinted with permission from [33]. Copyright (Journal of Applied Physics, 2012) AIP Publishing LLC.

4. GAS SENSING PROPERTIES OF PSiNWs

Several reports were presented using PSiNWs as das sensors. K. Q. Peng *et al.*[39] develop an economical method to fabricate n-PSiNWs assembly gas sensor. Figure 3(a) illustrates schematic diagram of the SiNWs gas sensor device structure. Two gold electrodes for electrical contacts were first deposited on the surface of the as-prepared PSiNWs samples by thermal evaporation or other methods through a mask; then two gold wires were connected to the golden electrodes via gold conductive adhesive. Gas sensing measurements were carried out by mounting the sensors in an air-tight test chamber in a flow-through manner and performed by monitoring the n-SiNWs assembly resistance under different NO concentrations in dry air at room temperature. NO is unstable in the air according to the following reaction: $NO+O_2 \leftrightarrow 2NO_2$; but the direct reaction is very low at low NO concentrations. Figures 3(b) and 3(c) show the dynamic electrical resistance response of the SiNW assembly sensor toward NO of various concentrations. $R/R_0 = R_0 - R/R_0$, where R_0 and R denote the PSiNWs assembly electrical resistance before and after NO exposure, respectively. It can be seen from Fig. 2 b that the electrical resistance of PSiNWs assembly was abruptly decreased by increasing the concentration of NO gas from 500 ppb to 100 ppm. By examining the sensor response to NO as a function of the concentrations, it was found that the as-prepared device shows swift response and recovery to low NO concentrations. The sensing response time for 500 ppb NO gas is about 30–40 s while the recovery time was about 60 s. The swift response can be attributed to the high surface-to-volume ratio of PSiNWs assembly.

In contrast, the rate of recovery was slower for higher NO concentrations; this can be understood as the thick porous nanowire layer leads to the slower desorption of large quantities of absorbed NO molecular from its high surface area porous surface.

Second application was developed by T. Q. N. Luong *et al.* [40] to detect low-concentration organic molecules detection via surface-enhanced Raman spectroscopy (SERS) effect using Ag nanoparticles-coated silicon nanowire arrays.The TEM images of representative SiNWs before and after AgNPs coating are shown in figures 4(a) and (b). From these images we can estimate that the diameters of SiNWs are in the region of 100–200 nm and can see clearly the AgNPs in the form of small black dots (with diameter in the 20–40 nm region) on the SiNW after Ag deposition. Here we can observe that the density of the AgNPs is relatively high and fairly evenly distributed across the entire surface of the SiNW.

To confirm the role of AgNPs in the SERS effect, authors have dropped aqueous MG (Malachit Green is an organic compound that is used as a dye for materials as silk) molecular solution onto the SiNW sample without AgNPs coating and after that performed the Raman measurements. The result (curve (d) of figure 4) shows that without AgNPs, the SERS effect did not occur. To demonstrate the superiority of the AgNPs-coated SiNW substrate in comparison with other types of substrate, the Raman measurements also have been performed after MG solution dropping on the AgNPs-coated porous silicon and flat silicon substrates. The results are also shown in figure 4 (curves (b) and (c)). Here, SERS signals from AgNPs-coated SiNW sample are much stronger than those from AgNPs-coated porous silicon (curve (b)) and flat silicon (curve (c)) samples. The increase of the Raman signals in the case of usingAgNPs-coated SiNW substrate; much higher density of the AgNPs is packed over a unit area of the substrate compared with porous silicon or flat silicon substrates which normally are used for SERS measurements [41]. The consequence of this is that the Raman signal increases many times. Moreover, according to the theoretical analysis [42], the characteristics of AgNPs coated on SiNWs, i.e., size, separation, and density, will provide an optimum environment for enhancement of Raman signals. The fact showed that the AgNPs cling tenaciously to the SiNWs, they do not fall off even if the SiNWs was subjected to an ultrasonic vibration. The characteristics of the substrate do not change even when it is exposed to the air for several months. It is worth remarking that in the case of AgNPs-coated SiNW substrate, in addition to enhancement of the individual Raman bands, the background signal is also increased. This rising of the baseline signal is partially attributed to inelastic light scattering by charge carrier excitations in Ag and partially attributed to fluorescence from Si nanowire arrays under the AgNPs [43].

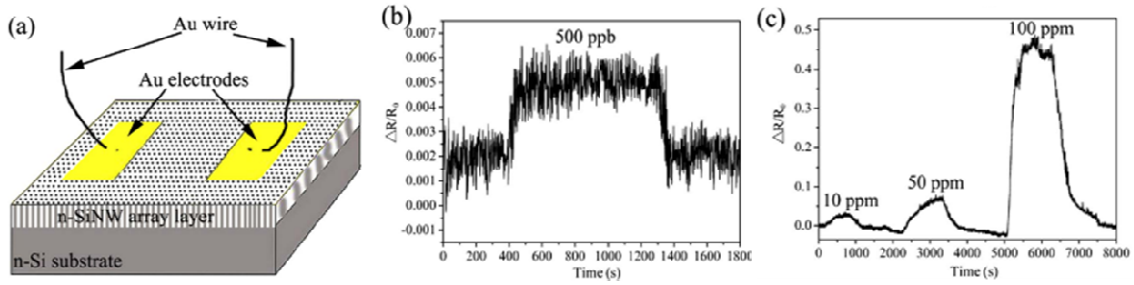

Figure 3.(a) Schematic illustration of the SiNWs gas sensordevice;**(b)**and**(c)** Dynamic electrical resistance responses of the SiNWgas sensor to NO in dry air at room temperature. The normalized electricalresistance change is plotted as a function of time with the sensor deviceexposed to NO concentrations from 500 ppb to 100 ppm.Reprinted with permission from [39]. Copyright (Applied Physics Letters, 2009) AIP Publishing LLC.

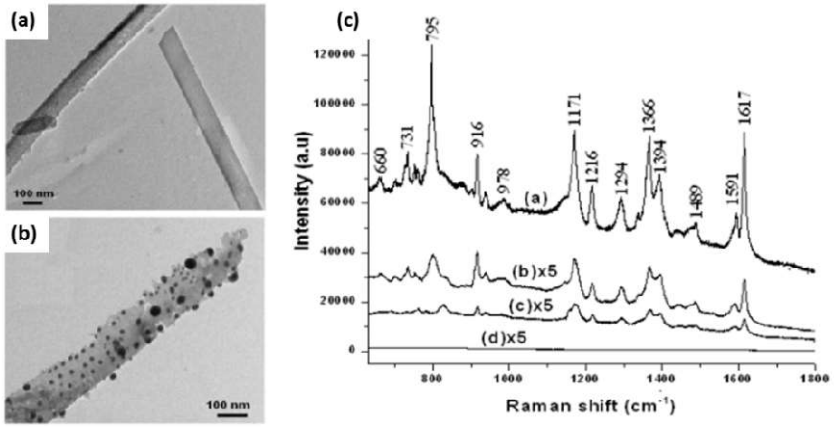

Figure 4.TEM images of some SiNWs before **(a)** and after **(b)**AgNPs deposition step.**(c)**Raman spectra of the samples dropped with 2×10^{-5}mol l^{-1} MG solution with different types of substrate: (a) AgNPs-coatedSiNWs; (b) AgNPs-coated porous silicon; (c) AgNPs-coated flat silicon and (d) uncoated SiNWs [40]. Copyright The Vietnam Academy Of Science And Technology (VAST). CC BY-NC-SA. Reproduced by permission of IOP Publishing.

5. CONCLUSIONS

In summary, this review report the structural properties of porous silicon nanowires (PSiNWs) fabricated using silver (Ag) ions assisted electroless etching method. The sensitivity of PSiNWs electrical properties to gaseous NOx at room temperature was demonstrated. Also, the results showed that the SERS-active substrates prepared by this method are excellent candidates for MG molecules sensing with high sensitivity, good reproducibility and excellent stability. The excellent sensing performance coupled with scalable synthesis of porous SiNWs could open up opportunities in scalable production of sensor chips working at room temperature.

6. REFERENCES

[1] Zhao X. Y., Wei C. M., Yang L., Chou M. Y., Quantum confinement and electronic properties of silicon nanowires, *Phys. Rev. Lett.*, 92, 236805, **2004**.

[2] Cui Y., Lieber C. M., Functional nanoscale electronic devices assembled using silicon nanowire building blocks, *Science*, 291, 851, **2001**.

[3] Lieber C. M., Wang Z. L., Functional nanowires, *MRS Bull*., 32, 99, **2007**.

[4] Najar A., Charrier J., Ajlani H., Lorrain N., Haesaert S., Oueslati M., Haji L., Optical gain at 1.53 µm in Er^{3+}–Yb^{3+} co-doped porous silicon waveguides, *Mater. Sci. Eng. B,* 146, 260, **2008.**

[5] Najar A., Lorrain N., Ajlani H., Charrier J., Oueslati M., Haji L., Er^{3+} doping conditions of planar porous silicon waveguides, *Appl. Surf. Sci.*, 256, 581, **2009.**

[6] Najar A., Ajlani H., Charrier J., Lorrain N., Haesaert S., Oueslati M., Haji L., Optical study of erbium-doped-porous silicon based planar waveguides, *Physica B.*, 396, 145, **2007.**

[7] Najar A., Charrier J., Lorrain N., Haji L., Oueslati M., Optical gain measurements in porous silicon planar waveguides codoped by erbium and ytterbium ions at 1.53 µm, *Appl. Phys. Lett.*, 91, 12, 121120-121120, **2007.**

[8] Najar A., Charrier J., Ajlani H., Lorrain N., Elhouiche H., Oueslati M., Haji L., Optical properties of erbium-doped porous silicon waveguides, *J. of Lumin.*, 121, 2, 245-248, **2006.**

[9]Najar A., Elhouichet H., Lorrain N., Oueslati M., Excitation mechanisms and localization sites of erbium-doped porous silicon, *Appl. Surf. Scien*., 252, 16, 5808-5813, **2006.**

[10] Koyama H., Nakagawa T., Ozaki T., Koshida N., Post-anodization filtered illumination of porous silicon in HF solutions: An effective method to improve luminescence properties, *Appl. Phys. Lett.*, 65, 1656**, 1994.**

[11] Canham L. T., Houlton M. R., Leong W. Y., Pickering C., Keen J. M., Atmospheric Impregnation of Porous Silicon At Room-Temperature,*J. Appl. Phys.*, 70, 422, **1991.**

[12] Huang Y., Duan X., Lieber C. M., Nanowires for integrated multicolor nanophotonics, *Small*, 1, 142, **2005.**

[13] Bohr M. T., Nanotechnology goals and challenges for electronic applications, *IEEE Trans. Nanotechnol.*, 1, 56, **2002.**

[14] Lieber C. M., One-dimensional nanostructures: chemistry, physics & applications, *Solid State Commun.*, 107, 607, **1998.**

[15] Xia Y. N., Yang P. D., Sun Y. G., Wu Y.,Mayers, N., Gates B., Yin Y., Kim F., Yan H., Large-scale synthesis and field emission properties of vertically oriented CuO nanowire films, *Adv. Mater.*, 15, 353, **2003.**

[16] Najar A., Gerland M., Jouiad M., Porosity-induced relaxation of strains in GaN layers studied by means of micro-indentation and optical spectroscopy, *J. of Appl. Phys.*, 111,9, 093513-093513, **2012.**
[17] Slimane A. B., Najar A., Elafandy R., San-Román-Alerigi D., Anjum D., Ng T. K., Ooi B. S., On the phenomenon of large photoluminescence red shift in GaN nanoparticles, *Nano. Res. Lett.*, 8, 342-348, **2013.**
[18] Slimane A.B., Najar A., Ng T. K.,Ooi B. S., Thermal Annealing Induced Relaxation of Compressive Strain in Porous GaN Structures,*Photonics Conference (IPC) IEEE*, 921–922, **2012.**
[19] Wagner R. S., Ellis W. C., The vapor-Liquid-Solid Mechanism of Crystal Growth and Its Application to Silicon, *Appl. Phys. Lett.*, 4, 89, **1964.**
[20] Morales A. M., Lieber C. M., A laser ablation method for the synthesis of crystalline semiconductor nanowires, *Science*, 279, 208, **1998.**
[21] Zhang Y. F., Tang Y. H., Wang N., Yu D. P., Lee C. S., Bello, I., Lee, S. T., Silicon nanowires prepared by laser ablation at high temperature, *Appl. Phys. Lett.,* 72, 1835, **1998.**
[22] Schubert L., Werner P., Zakharov N. D.,Gerth G., Kolb F. M., Long L., Geosele U., Tan T. Y., Silicon nanowhiskers grown on<111>Si substrates by molecular-beam epitaxy, *Appl. Phys. Lett.*, 84, 4968, **2004.**
[23] Stelzner T., Pietsch M., Andrea G., Falk F., Ose E., Christiansen S., Silicon nanowire-based solar cells., *Nanotechnology*, 19, 295203, **2008.**
[24] Lu M., Li M. K., Kong L. B., Guo X. Y., Li H. L., Silicon quantum-wires arrays synthesized by chemical vapor deposition and its micro-structural properties, *Chem. Phys. Lett.*, 374, 542, **2003.**
[25] Au F. C. K., Wong K. W., Tang Y. H., Zhang Y. F., Bello I., Lee S. T., Electron field emission from silicon nanowires, *Appl. Phys. Lett.*, 75, 1700, **1999.**
[26] Yu D. P., Lee C. S., Bello I., Sun X. S., Tang Y. H., Zhou G. W., Bai Z. G., Zhang Z., Feng S. Q., Synthesis of nano-scale silicon wires by excimer laser ablation at high temperature, *Solid State Commun.*, 105, 403, **1997.**
[27] Wang N., Tang Y. H., Zhang Y. F., Lee C. S., Bello I., Lee S. T., Si nanowires grown from silicon oxide, *Chem. Phys. Lett.*, 299, 237, **1999.**
[28] Juhasz R., Kylmeanen K., Galeckas A., Linnros J., Size-reduced silicon nanowires: Fabrication and electrical · characterization, *Mater. Sci. Eng.*, 25, 733, **2005.**
[29] Hochbaum A. I.,Gargas D., Hwang Y. J., Yang P., Single crystalline mesoporous silicon nanowires, *Nano Lett.*, 9, 3550, **2009.**
[30] Kumar D., Srivastava S. K., Singh P. K., Husain M., Kumar V., Fabrication of silicon nanowire arrays based solar cellwith improved performance, *Sol. Energy Mater. Sol.*, 95, 215-218, **2011.**
[31] Srivastava S. K., Kumar D., Singh P. K., Kar M., Kumar V., Husain M., Excellent antireflection properties ofvertical silicon nanowire arrays, *Sol. Energy Mater. Sol. Cells*, 94 1506–11, **2010.**
[32] Najar A., Charrier J., Pirasteh P., Sougrat R., Ultra-low reflection porous silicon nanowires for solar cell applications, *Optics Express*, 20, 16861-16870, **2012.**
[33] Najar A., Slimane A. B., Hedhili M. N., Anjum D., Sougrat R., Ng TK., Ooi B.S., Effect of hydrofluoric acid concentration on the evolution of photoluminescence characteristics in porous silicon nanowires prepared by Ag-assisted electroless etching method, *J. of Appl. Phys.*, 112, 033502-033502, **2012.**
[34] Peng K. Q., Yan Y. J., Gao S. P., Zhu J., Synthesis of Large-Area Silicon Nanowire Arrays via Self-Assembling Nanoelectrochemistry, *Adv. Mater.*, 14, 1164, **2002.**
[35] Qiu T., Wu X. L., Mei Y. F., Wan G. J., Chu P. K., Siu G. G., From Si nanotubes to nanowires: synthesis, characterization, and self-assembly, *J. Cryst. Growth*, 277, 143, **2005.**
[36] Zhong X., Qu Y., Lin Y. C., Liao L., Duan X., Unveiling the formation pathway of single crystalline porous silicon nanowires, *ACS Appl. Mater. Interfaces*, 3, 261–270, **2011.**
[37] Qu Y. Q., Liao L. , Li Y. J., Zhang H., Huang Y., Duan X. F., Electrically conductive and optically active porous silicon nanowires, *Nano Lett.*, 9, 4539, **2009.**
[38] Qu Y., Zhou H., Duan X., Porous silicon nanowires, *Nanoscale*, 3, 4060, **2011.**
[39]PengK. Q.,Wang X.,Lee S. T., Gas sensing properties of single crystalline porous silicon nanowires, *Appl. Phys. Lett.* 95, 243112, **2009.**
[40] Luong T. Q. N., Cao T. A., Dao T. C., Low-concentration organic moleculesdetection via surface-enhanced Ramanspectroscopy effect using Agnanoparticles-coated silicon nanowirearrays, *Adv. Nat. Sci.: Nanosci. Nanotechnol.* 4, 015018, **2013.**
[41] Shao M. W., Zhang M. L., Wong N. B., Ma D. D., Wang H., Chen W., Lee S. T., Ag-modified silicon nanowires substrate for ultrasensitive surface-enhanced Raman spectroscopy. *Appl. Phys. Lett.*, 93 233118, **2008.**
[42] Power A., Cassidy J., Betts T., Non Aggregated Colloidal Silver Nanoparticles forSurface Enhanced Resonance Raman Spectroscopy, *Analyst*, 136, 2794, **2011.**
[43] Yang Y., Meng G., Ag dendritic nanostructures for rapid detection of polychlorinated biphenyls based on surface-enhanced Raman scattering effect, *J. Appl. Phys.*, 107, 044315, **2010.**

7. ACKNOWLEDGEMENTS

None.